A Balanced Dual-Intracavity Dual-Mode Interlocking Method for Fiber Laser Self-Reference Wavelength Stabilization

Liuxin Zhang, Kang Ying, Guochao Wang, Haoyang Pi, Zhaoyong Wang, Yanguang Sun, Fang Wei, Youzhen Gui, Qing Ye, and Haiwen Cai, *Member, IEEE*

***Abstract*—The laser frequency stabilization technology is very important in the development of laser applications, and the improvement of this technology has tend to further expectations for portability and low cost, in addition to the realization of strict frequency control. In this context, we construct a dual-cavity laser frequency stabilization system based on an intracavity dual-mode self-reference mechanism. With this approach, we achieve remarkable results with a laser frequency drift of about 6.6 kHz and an Allen deviation (ADEV) of 10^{-13} levels over an integration time scale from 0.01 s to 1000 s. Notably, the solution achieves one of the best results without the need for an external reference structure. This work provides a way to realize wavelength-stabilized laser sources by interlocking two DFB lasers. This approach is distinguished by its simplicity and cost-effectiveness, making it a promising option for a variety of applications outside of the laboratory environment.**

***Index Terms*—Dual-mode, fiber lasers, laser noise, laser stability.**

I. Introduction

THE cutting-edge optical measurement field, encompassing high-resolution Lidar [1], [2], silicon-based photonics [3], [4], fiber optic sensing [5] and optical clock [6], [7], necessitate highly wavelength-stabilized laser sources. These experiments rely on the precision of the laser, meaning that wavelength stabilization accuracy is strictly required. Typically, sophisticated frequency stabilization design schemes are employed to meet their stringent demands, relying on optical or electrical feedback loops linked to an external frequency reference. These methods utilize elements such as Fabry-Pérot (FP) cavities [8], [9], absorption lines [10], and single photon wavelength modulation absorption [11] to achieve the desired stability. In this research field, current solutions utilizing FP cavities or WGM (Whispering-gallery mode) microcavities can achieve a wavelength stability criterion of ADEV within 100 ms, maintaining it at less than 10^{-15} [8]. However, these approaches are still susceptible to frequency stability issues due to thermal refractive noise and temperature variations on different time scales, primarily because of the presence of reference cavities [12]. To address the frequency drift caused by thermal noise, the concept of Ultra-Low Expansion (ULE) cavities has been proposed. Nevertheless, ULE cavity-stabilized lasers tend to have a bulky volume and lack of portability like WGM devices. Lately, beat-note locking techniques rooted in the intra-cavity dual-mode mechanism have emerged as a notable approach for laser wavelength stabilization. Through this method, laser frequency drift has been successfully curtailed to a mere 300 kHz per hour [13]. In a prior research endeavor of ours, we introduced an innovative technique aimed at mitigating wavelength drift in a distributed feedback (DFB) fiber laser. This novel approach harnesses the intracavity reference mechanism to achieve impressive results [14]. With locking the dual mode beat note frequency to a reference RF signal, it has good laser stability for integration time between 0.01s and 1000 s, the ADEV is about 10^{-13} level. However, frequency locking is traced back to an external RF signal, and the stabilization performance is basically restricted by the stability of the reference Rf source in these dual-mode temperature stabilization schemes. For the typical superior performance oscillator with ADEV 10^{-11}, the ADEV of laser wavelength stabilization results is between 10^{-13} and 10^{-12}. Although an atomic clock such as hydrogen clock can be used as a wavelength stabilization approach, it makes the laser system much more complicated and costly, which is unacceptable for the versatile application.

As far as we know, currently there was no reports about frequency stabilization method that did not require an external reference. In order to remove external limitation and achieve a more portable and low-cost structure while maintaining frequency stability results like external references, we optimize the

Manuscript received 5 January 2024; revised 23 January 2024; accepted 26 January 2024. Date of publication 30 January 2024; date of current version 19 February 2024. This work was supported in part by the National Key R&D Program of China under Grant 2023YFB2905300, in part by the National Natural Science Foundation of China under Grant U23A20379 and Grant 62175246, in part by the Natural Science Foundation of Shanghai under Grant 22ZR1471100, in part by Shanghai Rising-Star Program under Grant 22QB1406000, in part by the Strategic Priority Research Program of the Chinese Academy of Sciences under Grant XDB43000000, and in part by Youth Innovation Promotion Association CAS under Grant YIPA2021244. *(Corresponding author: Kang Ying.)*

Liuxin Zhang, Kang Ying, Haoyang Pi, Zhaoyong Wang, Yanguang Sun, Fang Wei, Youzhen Gui, Qing Ye, and Haiwen Cai are with the Key Laboratory of Space Laser Communication and Detection Technology, Shanghai Institute of Optics and Fine Mechanics, Chinese Academy of Sciences, Shanghai 201800, China (e-mail: lxzhang@siom.ac.cn; yingk0917@siom.ac.cn; hypi@siom.ac.cn; wzhy0101@siom.ac.cn; ygsun@siom.ac.cn; weifang@siom.ac.cn; yzgui@siom.ac.cn; yeqing@siom.ac.cn; hwcai@siom.ac.cn).

Guochao Wang is with the College of Intelligence Science and Technology, National University of Defense Technology, Changsha 410073, China (e-mail: wgc.19850414@163.com).

Digital Object Identifier 10.1109/JPHOT.2024.3360291

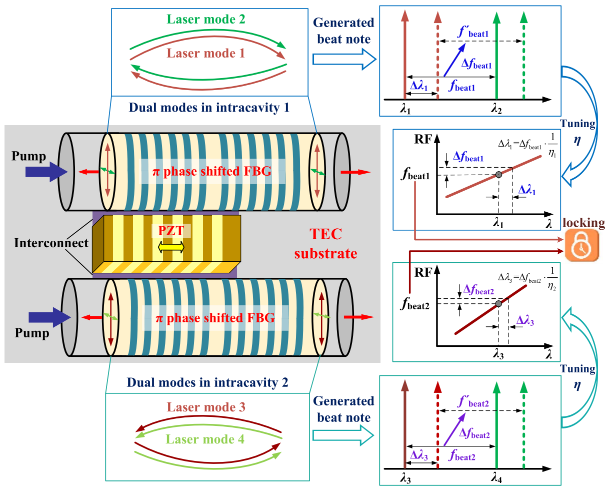

Fig. 1. Schematic of fiber laser wavelength stabilization based on BDIDM interlocking mechanism.

structure further from what we've done before. In this report, we demonstrate a novel self-reference wavelength stabilization method for fiber laser by using balanced dual intracavity dual mode (BDIDM) stabilization schemes. With establishing and self-locking the intracavity frequency reference signals of the two balanced dual-mode stabilization schemes, the laser wavelength drift can be realized without any external optical or electrical frequency reference, hence, the self-reference frequency stability is improved. Through our efforts, we have achieved a substantial reduction in laser wavelength drift, bringing it down from an initial 12 MHz ($\sim$ 0.1 pm) to less than 10 kHz. Remarkably, we have demonstrated a laser wavelength drift characterized by an ADEV at the exceptional 10^{-13} level for time between 0.01 s and 1000 s. [14]. The key strengths of our approach lie in its simple structure and good robustness. This innovation holds the potential in the realm of high-precision optical metrology, extending its reach beyond the confines of traditional laboratory settings.

II. Principle

A. Mapping of Beat-Note to Wavelength in a Single Intracavity

Because the wavelength of the DFB laser is determined by the refractive index (n) and the grating period (Λ), if an obvious birefringence effect is achieved by some way such as UV-induced birefringence, two orthogonal laser modes will be produced in the cavity [15]. Different laser wavelengths correspond to different refractive indexes, with a beat note frequency between them, which is shown in Fig. 1. The two wavelengths can be specifically presented as

$$\begin{cases} \lambda_1 = 2n_1\Lambda \\ \lambda_2 = 2n_2\Lambda \end{cases} \tag{1}$$

Therefore, based on formula (1), the beat note frequency f_{beat} can be deduced as

$$f_{\text{beat}} = \frac{c}{\lambda_1} - \frac{c}{\lambda_2} = \frac{c}{2n_1\Lambda} - \frac{c}{2n_2\Lambda} = \frac{c}{2\Lambda}\frac{n_2 - n_1}{n_1 n_2} \tag{2}$$

According to formulas (1) and (2), the change of refractive index n and grating period Λ will lead to the change of laser wavelength, while temperature (T) and strain (σ) will affect the refractive index due to thermo-optical and elastic-optic effects, meanwhile T and σ will lead to grating period changes. [12]. As a result, the laser wavelength drift ($\Delta\lambda_1$) appears due to T and σ, and the mathematical expression for $\Delta\lambda_1$ and Δf_{beat} are as follows:

$$\begin{cases} \Delta\lambda_1 = 2\left[\frac{\partial(n_1\Lambda)}{\partial X}\right]\Delta X = 2\left[\frac{\partial n_1}{\partial X}\Lambda + n_1\frac{\partial\Lambda}{\partial X}\right]\Delta X \\ \Delta f_{\text{beat}} = \frac{\partial f_{\text{beat}}}{\partial X}\Delta X = \frac{c}{2\Lambda^2 n_1 n_2}\left[(n_2 - n_1)\frac{\partial\Lambda}{\partial X}\right. \\ \qquad \left. + \Lambda\left(\frac{n_2\partial n_1}{n_1\partial X} - \frac{n_1\partial n_2}{n_2\partial X}\right)\right]\Delta X \end{cases} \tag{3}$$

where $X = T \text{ or } \sigma$. In this case, the laser wavelength drift $\Delta\lambda_1$ can be related to the frequency drift Δf_{beat} of the beat note in the intracavity, and be expressed as

$$\Delta\lambda_1 = \Delta f_{\text{beat}} \cdot \frac{1}{\eta} \tag{4}$$

where the correlation coefficient is summed as

$$\eta = \frac{c}{4\Lambda^2 n_1 n_2}\left[(n_2 - n_1)\frac{\partial\Lambda}{\partial X}\right. \\ \left. + \Lambda\left(\frac{n_2\partial n_1}{n_1\partial X} - \frac{n_1\partial n_2}{n_2\partial X}\right)\right] \Big/ \left(\frac{\partial n_1}{\partial X}\Lambda + n_1\frac{\partial\Lambda}{\partial X}\right) \tag{5}$$

It can be seen that η primarily relies on external interference sources affecting the laser wavelength, which encompass T and σ. Therefore, even if Δf_{beat} is identical, the wavelength variations induced by the two factors are different, resulting in a wavelength deviation in the terms of $\Delta f_{\text{beat}}(1/\eta_T - 1/\eta_\sigma)$. Evidently, it is crucial to make $\eta_T = \eta_\sigma$ for wavelength stabilization. According to the universal expression of η, η_σ and η_T can be deduced as

$$\begin{cases} \eta_\sigma = \frac{c}{4\Lambda^2 n_1 n_2}\left[(n_2 - n_1)\frac{\partial\Lambda}{\partial\sigma}\right. \\ \qquad \left. + \Lambda\left(\frac{n_2\partial n_1}{n_1\partial\sigma} - \frac{n_1\partial n_2}{n_2\partial\sigma}\right)\right] \Big/ \left(\frac{\partial n_1}{\partial\sigma}\Lambda + n_1\frac{\partial\Lambda}{\partial\sigma}\right) \\ \eta_T = \frac{c}{4\Lambda^2 n_1 n_2}[(n_2 - n_1)\frac{\partial\Lambda}{\partial T} \\ \qquad + \Lambda(\frac{n_2\partial n_1}{n_1\partial T} - \frac{n_1\partial n_2}{n_2\partial T})]/(\frac{\partial n_1}{\partial T}\Lambda + n_1\frac{\partial\Lambda}{\partial T}) \\ = \frac{c}{4\Lambda^2 n_1 n_2}[(n_2 - n_1)\frac{\partial\Lambda}{\partial T}\frac{1}{\Lambda} \\ \qquad + (\frac{n_2\partial n_1}{n_1\partial T} - \frac{n_1\partial n_2}{n_2\partial T})]/(\frac{\partial n_1}{\partial T} + n_1\frac{1}{\Lambda}\frac{\partial\Lambda}{\partial T}) \\ = \frac{c}{4\Lambda^2 n_1 n_2}[(n_2 - n_1)\varepsilon \\ \qquad + (\frac{n_2\partial n_1}{n_1\partial T} - \frac{n_1\partial n_2}{n_2\partial T})]/(\frac{\partial n_1}{\partial T} + n_1\varepsilon) \end{cases} \tag{6}$$

where ε is the equivalent thermal expansion coefficient of the laser cavity and denoted as $\partial\Lambda/\partial T \cdot 1/\Lambda$. From (5), it is feasible that the η_T can be made equal to η_σ through the regulation of ε. Consequently, achieving laser wavelength stability can be anticipated through the detection of the intracavity beat note signal frequency drift and subsequently locking this intracavity beat note signal. Moreover, the stabilized wavelength can be slightly tuned by change the reference beat frequency.

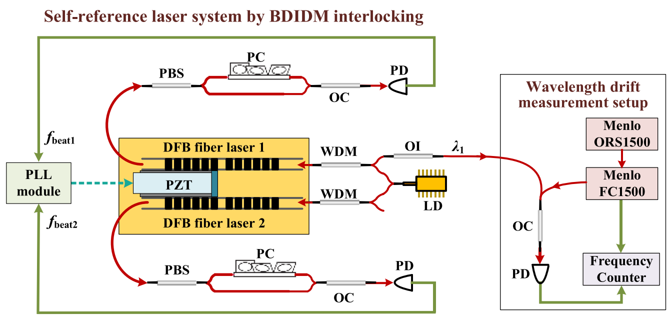

Fig. 2. Experimental setup: PBS (polarization beam splitter), OC (optical coupler), PD (photodetector), OI (optical isolator), LD (laser diode), PC (polarization controller), PLL (phase lock loop).

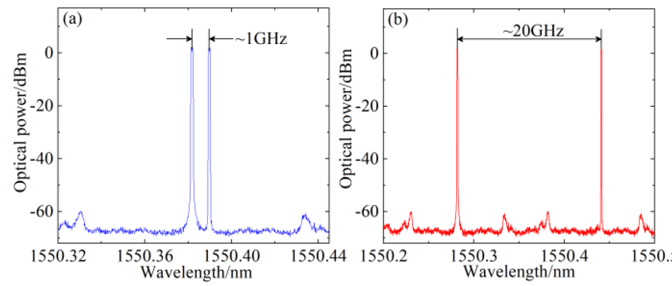

Fig. 3. Optical spectrum in the intracavity: (a) Spectrum of laser modes in intracavity 1. (b) Spectrum of laser modes in intracavity 2.

B. Balanced Beatnotes Interlocking of the Dual Intracavities

As depicted in Fig. 1, the whole laser system is built on a parallel and united dual intracavities, and they rely on the same slow thermal controlling structure on a TEC substrate. Moreover, the dual intracavities share the common piezoelectric (PZT) transducer, as is vital for wavelength modulation. When the two fiber lasers stretch the same PZT and impose the stress to the fiber cavity, the output wavelengths of the dual intracavities simultaneously bear their own variations, which are presented as

$$\begin{cases} \Delta\lambda_1 = \Delta f_{\text{beat1}} \cdot \frac{1}{\eta_1} = k_1 F \cdot \frac{1}{\eta_1} \\ \Delta\lambda_3 = \Delta f_{\text{beat2}} \cdot \frac{1}{\eta_2} = k_2 F \cdot \frac{1}{\eta_2} \end{cases} \tag{7}$$

where F is the efficient stress to PZT, k_1 and k_2 is the PZT modulation coefficient of the two intracavities, respectively. Naturally, through electronic locking, we can build the frequency relationship between f_{beat1} and f_{beat2}, namely

$$f_{\text{beat1}} = N f_{\text{beat2}} \tag{8}$$

Allowing for the existence of F, we define that $f_{\text{beat1}}(F) = f^0_{\text{beat1}} + \Delta f_{\text{beat1}}(F)$ and $f_{\text{beat2}}(F) = f^0_{\text{beat2}} + \Delta f_{\text{beat2}}(F)$, and therefore only for a specific condition that the stress F satisfies the equation

$$F = \frac{f^0_{\text{beat1}} - N f^0_{\text{beat2}}}{N k_2 - k_1} \tag{9}$$

two beat frequency variations induce by F can still maintain the relationship of (7). Ultimately, stable wavelength variations are obtained as

$$\begin{cases} \Delta\lambda_1 = k_1 \frac{f^0_{\text{beat1}} - N f^0_{\text{beat2}}}{N k_2 - k_1} \cdot \frac{1}{\eta_1} \\ \Delta\lambda_3 = k_2 \frac{f^0_{\text{beat1}} - N f^0_{\text{beat2}}}{N k_2 - k_1} \cdot \frac{1}{\eta_2} \end{cases} \tag{10}$$

Hence, through effectively locking the intracavity beat frequency f_{beat}, the wavelength drift is controlled.

III. Experimental Setup

To verify the laser wavelength stabilization effect derived from the aforementioned theory, in the subsequent sections, our experimental setup is outlined in Fig. 2. We use a 976 nm laser to pump two parallel fiber lasers, which operate at 1550 nm. According to the principle about inducing different laser modes, the resonators of both fiber laser 1 and fiber laser 2 are constructed by using the method of UV inscribing grating [15], [16]. Laser 1 use a π phase-shift grating whose birefringence characteristic δn_1 ($\delta n = (n_1 - n_2)/n_1$) is about 0.5×10^{-5}, which means the frequency difference between the two orthogonal polarization modes is up to GHz. Laser 2 adopts the same grating inscribing method as laser 1, but its birefringence characteristic δn_2 is larger. Using polarization controller (PC) to adjust the polarization state, there will be a beat note signals between the parallel polarization components of two laser modes for both fiber laser 1 and fiber laser 2, which could be detected to achieve the laser wavelength drift by a high-speed photodetector (Thorlabs RX25AF). With the PZT feedback which is synchronous to the two laser cavities, the laser wavelength drift for both fiber laser 1 and fiber laser 2 is compensated. Finally, the laser wavelength stabilization is realized by locking f_{beat2} to the other f_{beat1} using a phase lock loop module to drive the PZT, as is shown in Fig. 2. Besides, as described on the right of Fig. 2, devices are used to test the wavelength stability of the system, a commercial and ultra-precise frequency comb covering c-band optical wavelengths is used to measure the laser wavelength drift, by tracing the beat note between the laser in system and the used comb.

IV. Results and Discussion

A. The Regulation of η_T and η_σ

As to intracavity 1, δn_1 is about 0.5×10^{-5} induced by the UV inscribing process [15], [16], two orthogonal polarization modes with a signal to noise ratio (SNR) more than 60 dB exist, and their optical frequency gap is about 1 GHz, as is shown in Fig. 3(a). As to intracavity 2, δn_2 is about 1×10^{-4} for the PM fiber, the frequency difference is about 20 GHz, which is depicted in Fig. 3(b).

As described in the principles section above, the correlation coefficient η primarily relies on external interference sources affecting the laser wavelength, which encompass temperature (T) and strain (σ). The correlation coefficients due to temperature and strain are expressed as η_T and η_σ, respectively. Therefore, even if Δf_{beat} is identical, the wavelength variations induced by

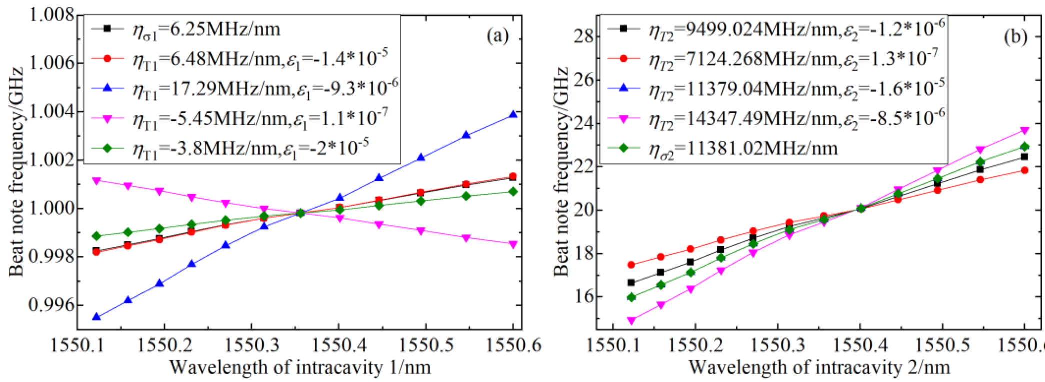

Fig. 4. Beat note frequency plotted against wavelength under various conditions: (a) Results of intracatity 1 for fiber laser 1. (b) Results of intracatity 2 for fiber laser 2.

the two factors are different, resulting in a wavelength deviation in the terms of $\Delta\lambda_{\text{error}} = (1/\eta_T - 1/\eta_\sigma)\Delta f_{\text{beat}}$, resulting in reduced wavelength stability.

According to formula (5), adjusting the laser cavity's equivalent thermal expansion coefficient, which denoted as $\varepsilon = \partial\Lambda/\partial T \cdot 1/\Lambda$, optimization of $\eta_T$can be realized. To achieve this, we have designed an intricate structure, the details of which have been elucidated in a prior publication [14]. It utilizes the disparate thermal expansion characteristics of Aluminum and Invar within the dual metal structure to control the change in the laser cavity length in response to temperature variations (i.e., equivalent thermal expansion coefficient). Subsequently, by adjusting the equivalent thermal expansion coefficient ε of the laser cavity for fiber laser 1, we conducted experimental measurements to assess the correlation coefficients (η_{T1}) and (η_{σ_1}) for various thermal expansion coefficient settings. The results of these measurements are depicted in Fig. 4(a). It can be seen that the η_{T1} match to the η_{σ_1} with thermal expansion coefficient $\varepsilon_1 = -1.4 \times 10^{-5}$. Also, the similar measurement is done for the PM fiber case, as is shown in Fig. 4(b), and the equal $\eta_{T_2}$and $\eta_{\sigma_2}$is achieved with thermal expansion coefficient $\varepsilon_2 = -1.6 \times 10^{-5}$.

Through adjusting ε for cavities of both fiber laser 1 and 2, we can observe the laser wavelength drift by keeping tabs on the beat note frequency. The temperature for fiber laser 1 and fiber laser 2 are controlled simultaneously by the same TEC, and the strain for fiber laser 1 and fiber laser 2 are controlled simultaneously by the same PZT. Then, the beat note frequency Δf_{beat_1} for fiber laser1 and the beat note frequency $\Delta f_{\text{beat}_2}$for fiber laser 2 are measured with modulating the controlled voltage of the PZT, as is shown in. Fig. 5. It can be seen that the beat note frequency $\Delta f_{\text{beat}_2}$is equal to 20 times of Δf_{beat_1} at a specific laser wavelength stabilization point.

Hence, according to formula (4), by converting the beat note into$20 \cdot \Delta f_{\text{beat}_1}$, the wavelength drift is effectively reduced. During the experimental procedure, we use an electronic phase lock device (Vescent D2-135) to lock the beat note Δf_{beat_2} to $20 \cdot \Delta f_{\text{beat}_1}$, as is shown in Fig. 5. And a PZT is used as feedback structure to compensate the laser wavelength drifts for both fiber laser 1 and fiber laser 2.

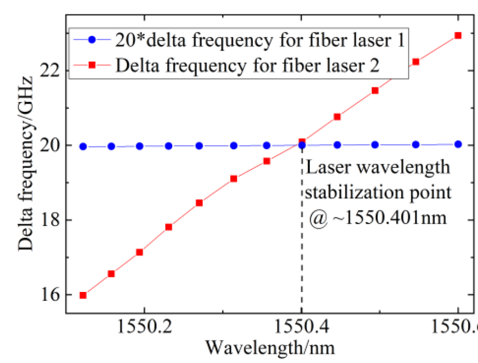

Fig. 5. Beat note frequency versus laser wavelength for interconnecting the fiber laser 1 and the fiber laser 2.

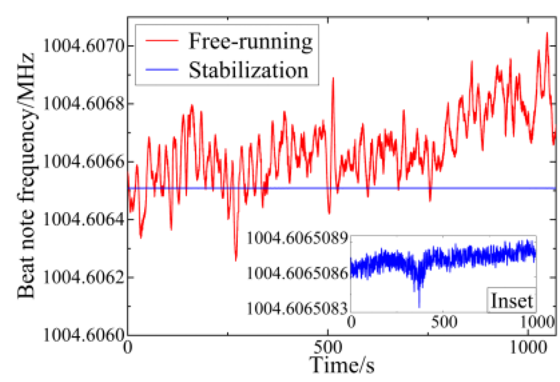

Fig. 6. Two-mode beat-note frequency stabilization results.

B. Interlocking of the Dual-Intracavity Beat Notes

See Fig. 5.

C. Laser Wavelength Stabilization Results

At first, the two-mode beat-note frequency Δf_{beat_1} fluctuations before and after the frequency stabilization are measured directly by a frequency counter (KEYSIGHT 53200) to examine the stabilization process, as is shown in Fig. 6. It can be seen

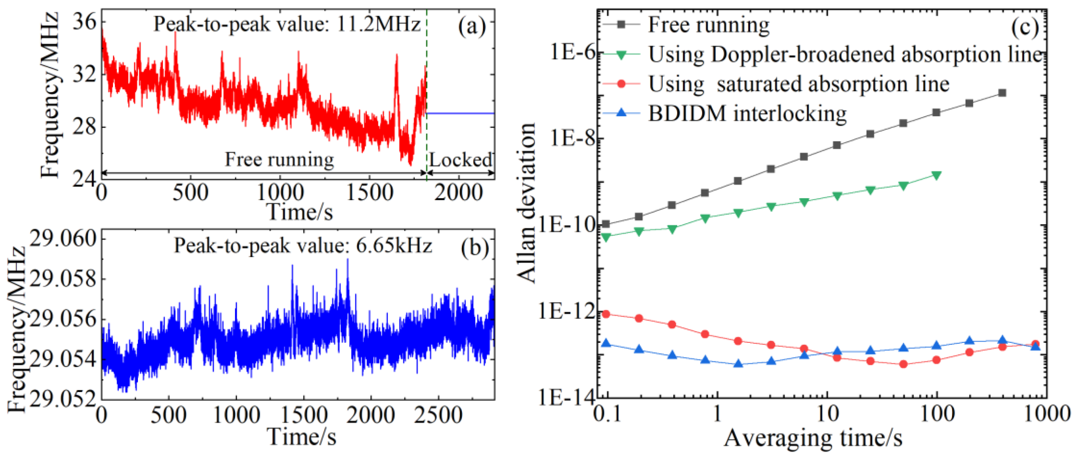

Fig. 7. Laser wavelength stabilization results: (a) Frequency drifts of beat note between the free-running fiber laser and the frequency comb. (b) Frequency drifts of beat note between the stabilized fiber laser and the frequency comb. (c) ADEVs by different experimental approaches.

that the peak to peak of the low beat-note frequency is reduce from 0.6 kHz to about 0.33 Hz, by a factor of about 1800. It should be noted that only the low beat-note frequency has been measured due to the bandwidth limitation of frequency counter, but the performance of one beat note is able to prove the locking and stabilization.)

For performance evaluation of the laser wavelength drift, we record the beat note frequency between the locked fiber laser 1 and a frequency comb which is atom-clock-referenced (Menlo FC1500 in Fig. 2.). Moreover, the mode-locked optical frequency comb is also stabilized to an ultra-stable maser laser (Menlo ORS1500 in Fig. 2.). The Menlo ORS1500 offers an ultra-narrow linewidth laser with excellent frequency stability. The core of the system is a highly detailed FP cavity made of ULE glass and operates in a vacuum at the zero thermal expansion point. At the point, the cavity length of the ULE cavity is very insensitive to changes in temperature and can be used as an optical reference source for optical frequency combs [17]. The Menlo ORS1500 system features a linear drift removal technique that eliminates baseline interference signals and accurately measures frequency drift. With this technique, a fractional instability ADEV is less than 1×10^{-14} for time between 0.01 and 1000 s can be achieved. Fig. 7(a) shows the drift results of the beat note between the fiber laser and the mentioned frequency comb, from the free running state to the stabilized state. The fluctuation of beat note frequency is recorded by a frequency counter (Keysight, 53230A). During a period of about 1800 s, the beat note frequency fluctuates within the range of from 24 MHz to 36 MHz, with a peak-to-peak value of 11.2 MHz. After the fiber laser turned to the locking mode, the beat note frequency results almost exhibit like a constant line in Fig. 7(a), showing very small frequency fluctuation. To observe a clear fluctuation of the beat note frequency for the stabilized laser, the beat note frequency results with a duration of about 2950 s are given in Fig. 7(b). It can be concluded that the laser wavelength drift is relate to the optical frequency comb has been dramatically reduced and tightly maintains within a peak-to-peak value of 6.65 kHz, which indicates that the proposed stabilizing method with BDIDM interlocking can successfully suppressed laser wavelength drift from a dozen of MHz level (corresponding to a wavelength drift of about 0.1 pm) to kHz level.

The data of wavelength drift are depicted in Fig. 6(c), In the subsequent sections, we provide the results obtained from both the free-running fiber laser and the laser stabilized using the BDIDM interlocking technique. The wavelength drift, quantified by ADEV achieved through BDIDM interlocking, reaches 10^{-13} for time between 0.01 s and 1000 s. As shown in Fig. 7(c), this method surpasses the free-running laser's performance at all integration time scales, especially, the ADEV is about one ten thousandth as free-running laser's at long integration time scales. Moreover, in Fig. 7(c), we have incorporated results that illustrate the conventional wavelength stabilization performance attained through absorption spectrum techniques. The typical wavelength stabilization performance using the Doppler-broadened absorption spectrum is 10^{-10} [18], our results is more than 2 order of magnitude better than it. The typical wavelength stabilitization performance in the integration time less than 10 s using the saturated absorption spectrum is about 10^{-12} [19], notably, our system exceeds the wavelength stability performance achieved by the former, especially for integration times less than 10 s. This signifies a promising avenue for realizing a frequency-stable laser source, offering an alternative to the traditional approach of locking lasers to absorption lines or FP cavities. Our approach stands out for its simplicity and effectiveness, lower cost feature. The current level of laser frequency stabilization is primarily limited by the residual difference η_T and η_σ. With further technical improvements such as using the laser wielding technique in the laser package process, we can expect to achieve a better performance at ADEV 10^{-15} level, which means that it can match the top frequency stabilization achieved by ULE cavity stabilized lasers.

V. Conclusion

In summary, a new self-reference laser wavelength stabilization technique is proposed by using BDIDM interlocking scheme for the first time. Our experimental study demonstrates a successful establishment of an intracavity frequency reference method and an effective feedback mechanism. Through the establishment and self-locking of the intracavity frequency reference signals within the two balanced dual-mode stabilization schemes, we achieve a significant reduction in laser frequency drift, resulting in a substantial improvement from its initial value 11.2 MHz to 6.6 kHz and ADEV at the 10^{-13} level across integration timescales ranging from 0.01 s to 1000 s. There are some improvements over long periods of time (10–1000 s) compared to our previous work. Additionally, there may be further performance improvements with the addition of anti-vibration to the system, especially when we want to apply it outdoors. These results hold significant importance, particularly in the transition of high-precision optical metrology applications, from the controlled laboratory environment to field deployments. Our approach offers the advantage of reduced complexity and enhanced robustness, facilitating the practical use of these precision instruments outside the laboratory setting.

References

[1] J. Ke et al., "Development of China's first space-borne aerosol-cloud high-spectral-resolution lidar: Retrieval algorithm and airborne demonstration," *PhotoniX*, vol. 3, no. 1, Dec. 2022, Art. no. 17, doi: 10.1186/s43074-022-00063-3.

[2] Y. Liu et al., "Eye-safe, single-frequency pulsed all-fiber laser for doppler wind lidar," *Chin. Opt. Lett.*, vol. 9, no. 9, pp. 090604–090607, 2011, doi: 10.3788/COL201109.090604.

[3] E. H. Bernhardi et al., "Ultra-narrow-linewidth, single-frequency distributed feedback waveguide laser in Al_2O_3:Er^3+ on silicon," *Opt. Lett.*, vol. 35, no. 14, Jul. 2010, Art. no. 2394, doi: 10.1364/OL.35.002394.

[4] J. - J. Chen et al., "Multi-wavelength injection locked semiconductor comb laser," *Photon. Res.*, vol. 10, no. 8, pp. 1840–1847, Aug. 2022, doi: 10.1364/PRJ.455165.

[5] A. Jderu, M. Enachescu, and D. Ziegler, "Mass flow monitoring by distributed fiber optical temperature sensing," *Sensors*, vol. 19, no. 19, Jan. 2019, Art. no. 19, doi: 10.3390/s19194151.

[6] S. A. Diddams et al., "An optical clock based on a single trapped ^{199} Hg $^{+}$ Ion," *Science*, vol. 293, no. 5531, pp. 825–828, Aug. 2001, doi: 10.1126/science.1061171.

[7] R. Le Targat et al., "Experimental realization of an optical second with strontium lattice clocks," *Nature Commun.*, vol. 4, no. 1, Jul. 2013, Art. no. 2109, doi: 10.1038/ncomms3109.

[8] T. Kessler et al., "A sub-40-mHz-linewidth laser based on a silicon single-crystal optical cavity," *Nature Photon.*, vol. 6, no. 10, pp. 687–692, Oct. 2012, doi: 10.1038/nphoton.2012.217.

[9] F. Wei et al., "Subkilohertz linewidth reduction of a DFB diode laser using self-injection locking with a fiber bragg grating fabry-perot cavity," *Opt. Exp.*, vol. 24, no. 15, pp. 17406–17415, Jul. 2016, doi: 10.1364/OE.24.017406.

[10] M. Scheller et al., "Externally refuelled optical filaments," *Nature Photon.*, vol. 8, no. 4, pp. 297–301, Apr. 2014, doi: 10.1038/nphoton.2014.47.

[11] F. Kéfélian, H. Jiang, P. Lemonde, and G. Santarelli, "Ultralow-frequency-noise stabilization of a laser by locking to an optical fiber-delay line," *Opt. Lett.*, vol. 34, no. 7, Apr. 2009, Art. no. 914, doi: 10.1364/OL.34.000914.

[12] A. B. Matsko, A. A. Savchenkov, N. Yu, and L. Maleki, "Whispering-gallery-mode resonators as frequency references I fundamental limitations," *J. Opt. Soc. Amer. B*, vol. 24, no. 6, Jun. 2007, Art. no. 1324, doi: 10.1364/JOSAB.24.001324.

[13] L. M. Baumgartel, R. J. Thompson, and N. Yu, "Frequency stability of a dual-mode whispering gallery mode optical reference cavity," *Opt. Exp.*, vol. 20, no. 28, Dec. 2012, Art. no. 29798, doi: 10.1364/OE.20.029798.

[14] K. Ying et al., "Ultra-stable fiber laser based on intracavity dual mode self-reference mechanism," *J. Lightw. Technol.*, vol. 40, no. 12, pp. 3923–3929, Jun. 2022, doi: 10.1109/JLT.2022.3149747.

[15] T. Erdogan and V. Mizrahi, "Characterization of UV-induced birefringence in photosensitive Ge-doped silica optical fibers," *J. Opt. Soc. Amer. B*, vol. 11, no. 10, Oct. 1994, Art. no. 2100, doi: 10.1364/JOSAB.11.002100.

[16] I. Bennion, J. A. R. Williams, L. Zhang, K. Sugden, and N. J. Doran, "Uv-written in-fibre bragg gratings," *Opt. Quantum Electron.*, vol. 28, no. 2, Feb. 1996, Art. no. 256420, doi: 10.1007/BF00278281.

[17] W. Zhao, H. Wu, Y. Fu, J. Ge, H. Yang, and S. Zhang, "Design of a transportable miniaturized optical reference cavity with flexibly tunable thermal expansion properties," *Front. Phys.*, vol. 10, Jan. 2023, Art. no. 1080196, doi: 10.3389/fphy.2022.1080196.

[18] C. Svelto, E. Bava, S. Taccheo, and P. Laporta, "Absolute frequency stabilization of two diode-pumped Er–Yb:Glass lasers to the acetylene P(15) line at 1534 nm," *Appl. Phys. Lett.*, vol. 73, no. 13, pp. 1778–1780, Sep. 1998, doi: 10.1063/1.122279.

[19] T. Talvard et al., "Enhancement of the performance of a fiber-based frequency comb by referencing to an acetylene-stabilized fiber laser," *Opt. Exp.*, vol. 25, no. 3, Feb. 2017, Art. no. 2259, doi: 10.1364/OE.25.002259.